Title	Capturing ultrafast quantum dynamics with femtosecond and attosecond x-ray core-level absorption spectroscopy.
Author(s)	Loh, Zhi-Heng.; Leone, Stephen R.
Citation	Loh, Z. H., & Leone, S. R. (2013). Capturing ultrafast quantum dynamics with femtosecond and attosecond x-ray core-level absorption spectroscopy. The Journal of Physical Chemistry Letters, 4(2), 292-302
Date	2012
URL	http://hdl.handle.net/10220/17347
Rights	© 2012 American Chemical Society. This is the author created version of a work that has been peer reviewed and accepted for publication by The Journal of Physical Chemistry Letters, American Chemical Society. It incorporates referee's comments but changes resulting from the publishing process, such as copyediting, structural formatting, may not be reflected in this document. The published version is available at: [http://dx.doi.org/10.1021/jz301910n].

Capturing Ultrafast Quantum Dynamics with Femtosecond and Attosecond X-Ray Core-Level Absorption Spectroscopy

Zhi-Heng Loh[1] and Stephen R. Leone[2,*]

[1] Division of Chemistry and Biological Chemistry, and Division of Physics and Applied Physics, School of Physical and Mathematical Sciences, Nanyang Technological University, Singapore 637371, Singapore

[2] Departments of Chemistry and Physics, University of California, and Chemical Sciences Division, Lawrence Berkeley National Laboratory, Berkeley, California 94720, USA

Abstract

Recent technical advances in ultrafast laser sources enable the generation of femtosecond and attosecond soft x-ray pulses in tabletop laser setups as well as accelerator-based synchrotron and free-electron laser sources. These new light sources can be harnessed via pump-probe spectroscopy to elucidate ultrafast quantum dynamics in atoms, molecules, and condensed matter with unprecedented time resolution and chemical sensitivity. Employing such ultrashort pulses in transient x-ray absorption spectroscopy combines the unique advantages of core-level absorption probing of chemical environments and oxidation states with the ability to obtain ultimately freeze-frame snapshots of electronic and nuclear dynamics. In this Perspectives Article we provide an overview of the progress in applying the recently developed technique of femtosecond to attosecond time-resolved soft x-ray transient absorption spectroscopy to the study of ultrafast phenomena, including some of our own efforts to elucidate the interaction of intense laser pulses with atoms and molecules in the strong-field, nonperturbative limit. Possible avenues for future work are outlined.

[*] Corresponding author. Electronic mail: srl@berkeley.edu

TOC graphic

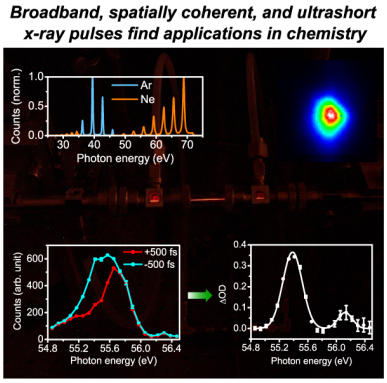

Keywords: Time-resolved x-ray absorption spectroscopy, high-order harmonic generation

With its origin in the flash photolysis technique invented by Norrish and Porter,[1] transient absorption spectroscopy is perhaps the most widely used and most basic technique among the assortment of ultrafast pump-probe methods.[2] This method utilizes a pump pulse to initiate a transformation in a sample that is interrogated after a variable time delay by recording the differential absorption of a probe pulse.[3–5] The time-evolution of the transient absorption spectra elucidates the temporal behavior and the internal energy level structure of the ephemeral species that are produced by the interaction of the pump pulse with the sample.

Advances in nonlinear optics along with the emergence of synchrotron and free-electron laser light sources now offer ultrashort light pulses that can be tuned from the terahertz[6] to the hard x-ray,[7] enabling transient absorption spectroscopy to examine how various quantum mechanical degrees of freedom of a sample – rotational, vibrational, and electronic – respond to transformations induced by the pump pulse. Furthermore, remarkable progress over the past several decades in the generation and manipulation of ultrashort laser pulses[8,9] now enables pulses that comprise a mere few cycles of the electric field to be employed in experiments. The use of such pulses, such as the sub-5-fs output furnished by visible noncollinear optical parametric amplifiers,[10] yields transient absorption data with sub-10-fs time resolution.[11] These advantages, along with the ability to yield quantitative information such as relative populations, coherence and phase information, and absorption cross-sections, enable the broad application of transient absorption spectroscopy to the investigation of important ultrafast phenomena that occur in physics, chemistry, materials science, and biology.

While the utilization of terahertz, infrared, visible, and ultraviolet femtosecond pulses for time-resolved transient absorption spectroscopy is relatively well-established, it is only very recently that similar experiments have been performed with x-ray pulses. In time-resolved x-ray absorption spectroscopy, the differential absorption of core-level electron transitions is recorded as a function of probe photon energy and pump-probe time delay. The absorption of an x-ray photon results in the promotion of a core-level electron either to an unoccupied valence orbital or into the continuum (Figure 1).[12] The spectrally distinct core-level absorption edges allow

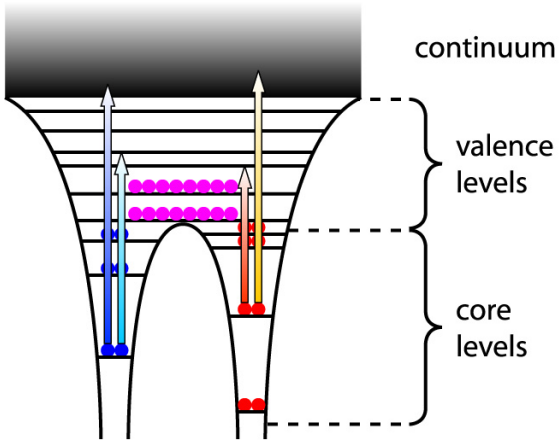

Figure 1. Transitions in x-ray absorption spectroscopy originate from the promotion of electrons in the core levels either to unoccupied valence levels or to the continuum. Possible x-ray absorption transitions for a heteronuclear diatomic molecule are shown here. Probing of the core levels offers element specificity, whereas participation of the valence levels in x-ray absorption confers a high degree of sensitivity to the valence electronic structure.

element-selective detection of ultrafast dynamics. X-ray absorption near-edge spectra (XANES), which are recorded in the vicinity of an absorption edge, are sensitive to changes in the valence electronic structure, whereas extended x-ray absorption fine-structure spectra (EXAFS), which are recorded at photon energies beyond the absorption edge, directly reveal changes in interatomic distances. Time-resolved x-ray absorption spectroscopy therefore tracks the temporal evolution of the valence electronic structure and/or molecular geometry of the various atomic constituents present in the transient species produced by photoexcitation.

Prior to the arrival of femtosecond x-ray sources, picosecond to nanosecond time-resolved x-ray absorption spectroscopy was performed by directly employing, for example, the ~100-ps x-ray pulses from synchrotrons.[13,14] These investigations elucidate the rich photophysics and excited-state nuclear reorganization of transition metal complexes via both XANES and EXAFS spectroscopies. Pioneering work on tabletop laser-produced plasmas also enabled the application of picosecond x-ray pulses produced by these sources to ultrafast x-ray absorption spectroscopy.[15,16]

The recent advent of femtosecond and attosecond x-ray pulses now allows time-resolved x-ray absorption to approach time scales that are commensurate with nuclear and even electronic motion. Femtosecond x-ray pulses are produced at both large-scale accelerator-based facilities as well as on tabletop laser-based setups. In the case of the former, femtosecond pulse slicing of electron bunches in a third-generation synchrotron storage ring[17] and temporal compression of electron bunches at free-electron lasers[18,19] yield both soft ($E_\gamma < 1$ keV) and hard ($E_\gamma > 1$ keV) x-ray pulses with durations that are as short as a few femtoseconds, with attosecond pulses on the horizon.[20] In tabletop setups, the irradiation of a high-Z metal target by an intense femtosecond laser pulse produces a plasma at the surface of the metal target from which bremsstrahlung femtosecond hard x-ray pulses are emitted.[21,22] Alternatively, soft x-ray pulses can be produced by driving radiative electron-ion recombination coherently in a process known as high-order harmonic generation (HHG).[9,23] The periodicity and extreme nonlinearity of the HHG process results in a train of attosecond soft x-ray pulses phase locked to the driving laser field.[24] The resultant comb of harmonics, after suitable monochromatization,[25] presents itself as an attractive photoionization light source for photoelectron spectroscopy.[26–28] Moreover the use of carrier-envelope phase-stabilized, few-cycle driving laser pulses yields, after appropriate spectral high-pass filtering of the HHG output, isolated attosecond pulses[29] in the soft x-ray that can be used to probe ultrafast dynamics with unprecedented time resolution.[30] Further extension of the HHG output into the hard x-ray promises to deliver pulses of zeptosecond duration (1 zs = 10^{-21} s) in the not-so-distant future.[23]

The method of choice for generating the ultrashort x-ray pulse depends on the problem at hand. HHG yields soft x-ray pulses in the range of 0.01 – 1 keV. Soft x-ray light in the tens of electron volt range, where the photon flux can be as high as 10^{14} photons per second in 1% bandwidth,[31,32] can be used to probe inner-valence and outer-core level transitions. In addition to the high photon flux, the relatively large photoabsorption cross-sections further enhances the count rates for experiments performed in this photon energy range. The exquisite time resolution that is offered by attosecond pulses produced via HHG further enhances the attractiveness of

such a light source. Due to the limited absorption lengths at these low energies, however, investigations with HHG light sources are limited to gas phase samples and ultrathin foils. Femtosecond pulse slicing, laser-produced plasmas, and x-ray free-electron lasers offer higher x-ray photon energies that extend to ~10 keV. The spatially confined nature of core-levels probed at such high energies allows the direct retrieval of structural information via extended x-ray absorption fine structure (EXAFS). Moreover, the reasonably high transmission of these hard x-rays through solvents, window materials, or even air itself at these photon energies not only simplifies the vacuum requirements of experimental setups, but also allows measurements on solutions in lithographically prepared nanofluidic flow cells. These flow cells allow studies, including those in the soft x-ray, to be performed on liquids and solution samples.[33] Unfortunately these high-energy sources are not without technical challenges. The spatially incoherent nature of x-rays emitted from a laser-produced plasma translates to a low photon collection efficiency from the source, and slicing of ~100-ps electron bunches by ~100-fs laser pulses leads to a relatively low flux in the femtosecond x-ray pulse. Both factors result in a low x-ray photon flux at the sample target (10^3 photons per pulse per 1 keV bandwidth for laser-produced x-rays[34] and $10^2 - 10^3$ photons per pulse per 0.1% bandwidth for pulse slicing[17,35]). X-ray free-electron lasers, which provide remarkable millijoule-level pulse energies in the hard x-ray, require exquisite synchronization between the optical laser and the x-ray free-electron laser. The current electro-optic sampling scheme for determining the pump-probe time delay yields timing jitters of <10 fs,[36] which needs further improvement before few-femtosecond pump-probe measurements will be possible.

This Perspectives Article will focus on some of the recent progress in employing femtosecond and attosecond x-ray pulses to investigate ultrafast electron and nuclear dynamics in atoms, molecules, and condensed matter via core-level transient absorption spectroscopy. Brief updates on experiments performed with this emerging technique at synchrotrons and free-electron lasers will also be provided.

The earliest application of HHG-produced light to femtosecond time-resolved soft x-ray absorption spectroscopy was reported by Nakano and co-workers.[37] In that work, the intense near-infrared (NIR) output from an amplified femtosecond Ti:sapphire laser system was used to drive the sequential ionization of neutral Kr atoms to Kr^{2+}. The formation of the transient Kr^{+} species was detected by the depletion of the 51st harmonic of the Ti:sapphire laser output at 15.6 nm when the NIR and soft x-ray pulses overlap in time. Resonant absorption by Kr^{+} at this wavelength results from the $^2P_{3/2} \rightarrow {}^2D_{5/2}$ transition, in which a 3*d* core-level electron is promoted to the vacancy in the 4*p* valence shell. Assuming a sech^2 envelope for the soft x-ray pulse, the pulse duration was determined to be 220 fs full-width at half-maximum (FWHM). This approach to NIR-soft x-ray cross-correlation was applied earlier by the same group to characterize picosecond soft x-ray pulses produced by intense laser irradiation of a tungsten metal target,[38] and it was recently employed to measure the pulse duration of hard x-ray light (14.3 keV photon energy) produced at a synchrotron.[39]

At Berkeley, femtosecond soft x-ray transient absorption spectroscopy was first used to explore the interaction of atoms and small molecules with intense femtosecond laser pulses, with recent extensions to weak-field, single-photon excitation of small molecules and thin films. The availability of high intensity laser pulses provides strong impetus for studying the interaction of intense laser pulses with atoms and molecules,[9,40] which is emphasized here. As the laser electric field strength approaches the effective potential experienced by a valence electron in the presence of the other electrons and the ion core ($\sim 10^8$ V/cm), a significant distortion of the atomic potential can be induced by the intense laser pulse. Under such conditions, a description of light-matter interaction within the framework of time-dependent perturbation theory is no longer adequate, and a nonperturbative treatment becomes necessary. This transition signifies the emergence of the strong-field regime. Following a brief description of the experimental apparatus based on HHG-produced femtosecond soft x-ray pulses, three different classes of strong-field experiments performed with the setup will be outlined. These experiments yield

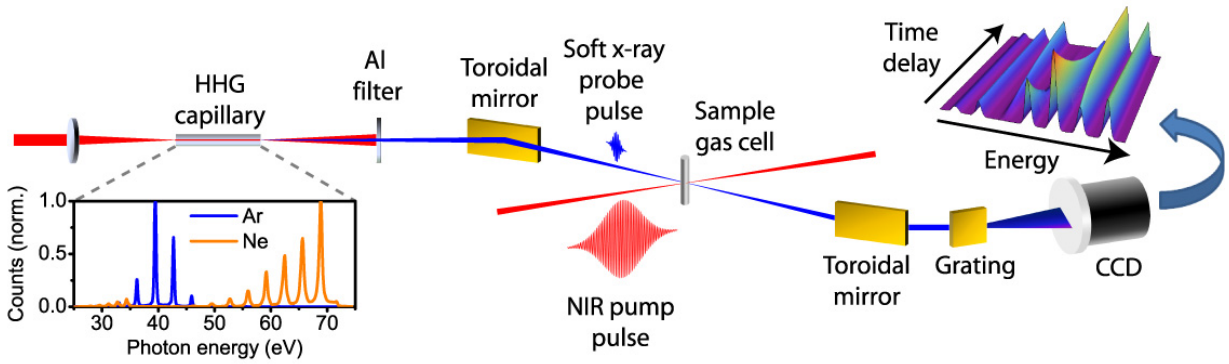

Figure 2. Schematic illustration of the first-generation apparatus for femtosecond time-resolved soft x-ray transient absorption spectroscopy constructed in Berkeley. Soft x-ray pulses produced by high-order harmonic generation in a capillary filled with Ar or Ne are refocused by a toroidal mirror into the sample target, where it intersects an optical pump pulse. The transmitted soft x-ray pulse is spectrally dispersed in a home-built soft x-ray spectrometer equipped with a CCD camera. Typical spectra for the soft x-ray light produced by HHG are shown.

some of the earliest information on state-resolved populations and dynamics in strong-field phenomena.

A schematic illustration of the first-generation tabletop soft x-ray transient absorption apparatus in Berkeley is shown in Figure 2.[41] Femtosecond soft x-ray pulses are produced by focusing part of the NIR output from an amplified Ti:sapphire laser system into a 150-μm-diameter capillary filled with argon or neon; the remaining portion of the laser output serves as the optical strong-field pump pulse. In recent versions, a semi-infinite gas cell is used for the harmonic generation step. The soft x-ray photons span the energy range of, for example, 40 – 73 eV, in which the high-energy cut-off originates from the $L_{2/3}$ absorption edge of the aluminum filters that are used to reject the residual NIR driving laser light. A gold-coated toroidal mirror refocuses the quasi-continuous HHG emission into the sample target gas cell, after which the transmitted soft x-ray light is spectrally dispersed in a home-built spectrometer equipped with an x-ray CCD camera. Such a configuration in which spectral dispersion occurs only after the sample is easy to implement, guarantees the best possible time resolution by minimizing temporal distortion of the soft x-ray pulse, and allows simultaneous observation of multiple

species absorbing at different probe energies. Due to the small absorption lengths of window materials in the soft x-ray and the high-intensity optical pump beams required, a quasi-static gas cell is employed as the sample target, in which 200-μm-diameter pinholes drilled through the wall of the gas cell allow transmission of the pump and probe beams. The sample gas density, which can be inferred from nonresonant absorption by the sample, can be as high as $>3 \times 10^{18}$ cm^{-3}. The optical pump beam is focused into the sample where it intersects the soft x-ray probe beam in a noncollinear geometry. A half-waveplate – polarizer combination allows control over the polarization axis and energy of the pump pulse. Typical peak intensities employed in the experiments range from $\sim 10^{13} - 10^{15}$ W/cm^2, which correspond to peak electric field amplitudes of $\sim 10^8 - 10^9$ V/cm.

New information about the strong-field ionization of Xe atoms is obtained by utilizing the soft x-ray transient absorption spectrometer described above to characterize the $|j, m\rangle$ quantum state-resolved distribution of the resultant Xe^+ ions (Figure 3).[42] Previous experiments gave conflicting results regarding the existence of hole orbital alignment in photoions produced by strong-field ionization of noble gases.[43,44] In the first Berkeley work, the $^2P_{3/2} \rightarrow {}^2D_{5/2}$ and $^2P_{1/2} \rightarrow {}^2D_{3/2}$ transitions of Xe^+ ions at the $N_{4/5}$ ($4d$) edge are resolved in the transient absorption spectrum, thereby yielding the population ratio of the two spin-orbit states of Xe^+. The $^2P_{3/2} \rightarrow {}^2D_{3/2}$ transition is characterized in recent work.[45] The non-vanishing polarization anisotropy measured for the $^2P_{3/2} \rightarrow {}^2D_{5/2}$ probe transition provides direct evidence that the $^2P_{3/2}$ state is significantly aligned, in agreement with other recent results obtained by laser-pump synchrotron-probe measurements on Kr^+ ions, also produced by strong-field ionization.[44,46] The degree of alignment yields the shape of the hole density of the Xe^+ ions. Comparison of the experimentally reconstructed hole density with that obtained from tunnel ionization calculations[47] suggests that the electrons undergoing strong-field ionization do not respond instantaneously to the laser field. That is, the interaction of the Xe atom with the ionizing laser field is not completely adiabatic (quasi-static). Under such circumstances, the ionizing electron experiences a modification in the shape of the atomic potential as it escapes from the atom on the half-cycle time scale and is

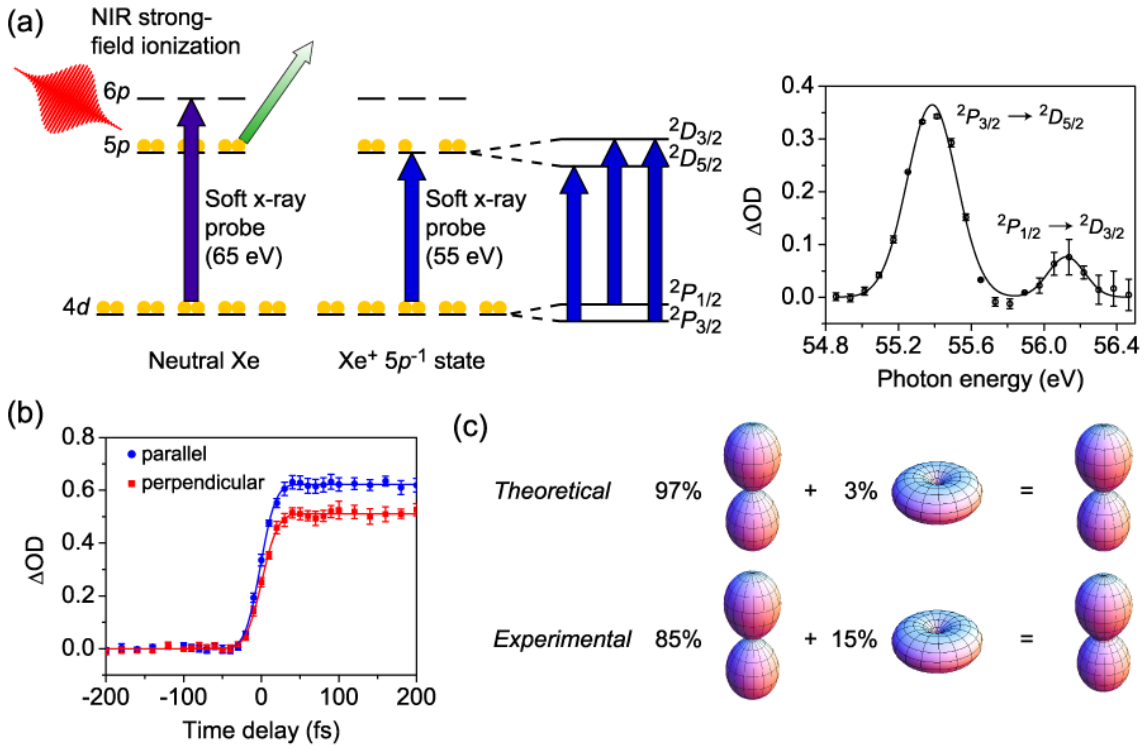

Figure 3. State-resolved soft x-ray absorption probing of Xe^+ ions produced by strong-field ionization. (a) In a neutral Xe atom, the lowest energy dipole-allowed transition from the 4*d* core level is the $4d \rightarrow 6p$ transition at ~65 eV. Ejection of a 5*p* valence electron from Xe gives rise to a new $4d \rightarrow 5p$ transition that is located at ~55 eV. Spin-orbit coupling splits the $5p^{-1}$ valence state into the $^2P_{1/2}$ and $^2P_{3/2}$ states, whereas the $4d^{-1}$ probe final state is split into the $^2D_{3/2}$ and $^2D_{5/2}$ states. The allowed x-ray transitions between these two sets of states are illustrated. The $^2P_{3/2} \rightarrow {}^2D_{5/2}$ and $^2P_{1/2} \rightarrow {}^2D_{3/2}$ transitions are shown in the experimental transient absorption spectrum. (b) The observed polarization anisotropy at the $^2P_{3/2} \rightarrow {}^2D_{5/2}$ transition shows that the $^2P_{3/2}$ state is aligned. (c) The alignment distribution obtained from tunnel ionization calculations with the inclusion of spin-orbit coupling is shown in the top panel. The hole density distribution obtained from experiment is shown in the bottom panel.

therefore sensitive to the internal structure of the atom. This result is supported both by multiphoton Floquet calculations and by the previous observation of Freeman resonances in photoelectron spectra collected under similar experimental conditions.[48] Atomic strong-field ionization is further investigated through the observation of coherences between Kr ion states by the extension of this type of experiment into the attosecond time domain (see below).

In a different type of experiment, the laser-dressing of helium double excitation states is used to explore coherent optical phenomena in the soft x-ray.[49] Coherent optical phenomena,

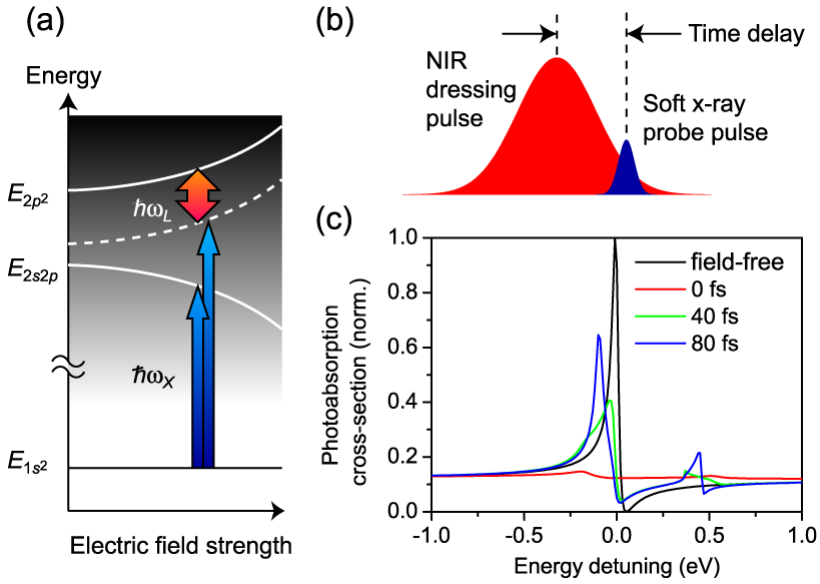

Figure 4. (a) Coherent coupling of the $2s2p$ ($^1P^o$) and $2p^2$ ($^1S^e$) double excitation states of He by an 800-nm dressing laser field results in the formation of an Autler-Townes doublet. The $2s2p$ and $2p^2$ states are located 60.15 eV and 62.1 eV, respectively, above the $1s^2$ ground state. The shaded region depicts the $1s\varepsilon l$ continuum, located 24.59 eV above the $1s^2$ ground state. ω_L and ω_X represent the frequencies of the dressing laser and soft x-ray probe, respectively. (b) The considerably shorter duration of the soft x-ray probe pulse (<13 fs) compared to the dressing laser pulse (45 fs) allows different dressing field strengths to be sampled by varying the time delay between the two pulses. (c) Simulated soft x-ray absorption spectra of He in the vicinity of $2s2p$ line as a function of time delay between the NIR dressing laser pulse and the soft x-ray probe pulse. The field-free Fano lineshape is also shown.

such as electromagnetically induced transparency,[50] offer the exciting possibility of extending amplitude and spectral phase shaping techniques into the soft x-ray.[51] The He $2s2p$ ($^1P^o$) and $2p^2$ ($^1S^e$) double excitation states are examined in this work; the former is accessible from the ground state via a dipole-allowed transition and appears as a Fano lineshape at 60.15 eV due to interference between the direct ionization and autoionization pathways (Figure 4).[52,53] The experiment employs an 800 nm laser pulse to coherently couple the two double excitation states, and the resultant Rabi flopping between the two autoionizing states is observed via soft x-ray transient absorption spectroscopy. The considerably shorter soft x-ray pulse (<13 fs)[41] compared to the 800-nm dressing pulse (45 fs) allows the dressing field strength to be varied simply by changing the time delay between the two pulses. The transient absorption spectra acquired at

different time delays reveal the presence of an Autler-Townes doublet that is associated with electromagnetically induced transparency. Theoretical simulations successfully reproduce these experimental results. Recently the use of synchrotron-produced femtosecond x-ray pulses allowed the extension of coherent optical phenomena to ~keV photon energies.[54] In that work, coherent coupling of the Ne $1s^{-1}3p^1$ and $1s^{-1}3s^1$ states by an 800-nm femtosecond laser pulse results in an increase in the transparency of the neon $1s \rightarrow 3p$ transition at 867 eV by up to a factor of ~3. The change in x-ray transparency as a function of time delay between the x-ray probe pulse and the NIR dressing pulse is used to cross-correlate the two pulses, from which an x-ray pulse duration of 250 fs FWHM was retrieved. Taking advantage of a close resonance of 800 nm light between transiently probed Xe 6*p* states and neighboring states, Autler-Townes splitting with multiple branches are observed when the Rabi frequencies exceed the laser frequency.[45,55]

Turning to molecular dynamics, femtosecond soft x-ray transient absorption spectroscopy is utilized to observe the ultrafast dynamics that are involved in the strong-field dissociative ionization of small molecules.[56] The interaction of nonresonant strong-laser fields with molecules provides a widely applicable route for ionizing molecules and manipulating chemical reaction pathways.[57,58] A time-domain perspective of dissociative ionization that is offered by femtosecond soft x-ray absorption spectroscopy complements the numerous measurements of photofragment ion yields as a function of laser peak intensity.[59] The soft x-ray transient absorption spectrum recorded in the vicinity of the Br $M_{4/5}$ (3*d*) edge after strong-field ionization of CH_2Br_2 reveals the richness of the dissociative ionization process (Figure 5). At an 800-nm laser pulse peak intensity of 6×10^{14} W/cm^2, sequential double ionization of CH_2Br_2 to form the metastable $CH_2Br_2^{2+}$ dication is observed. At a lower laser peak intensity of 2×10^{14} W/cm^2, the presence of the $CH_2Br_2^+$ parent ion, the CH_2Br^+ fragment ion, as well as the Br atom in both $^2P_{3/2}$ (Br) and $^2P_{1/2}$ (Br*) states are observed. The appearance time scales for Br and Br* are different, 130 ± 22 fs and 74 ± 10 fs, respectively (Figure 5). The shorter appearance time for the spin-orbit-excited Br* atom cannot be rationalized by the production of Br and Br* from a single

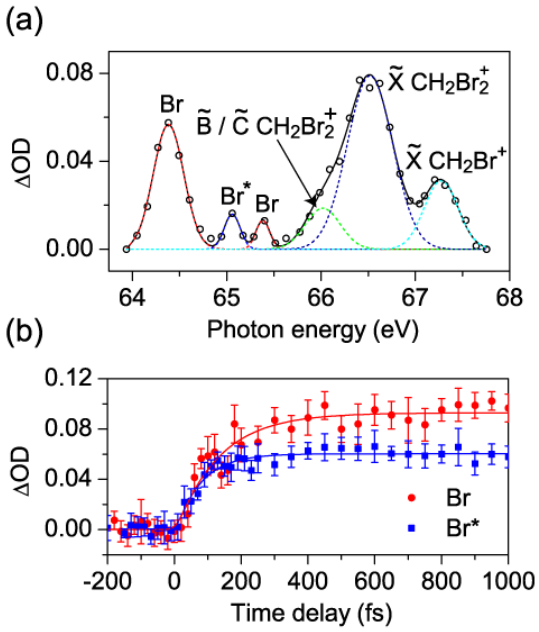

Figure 5. (a) The soft x-ray transient absorption spectrum recorded after strong-field dissociative ionization of CH_2Br_2 at a laser peak intensity of 2×10^{14} W/cm^2 reveals a variety of photofragments in addition to the $CH_2Br_2^+$ parent ion. (b) State-resolved probing of the Br photofragments shows the counterintuitive slower appearance of the Br atom as opposed to the spin-orbit-excited Br* atom. This observation suggests that field-dressed states are involved in the C—Br bond dissociation.

dissociative state.[60] Even though the exact mechanism for dissociation is unidentified, it is important to note that, given the comparable ionizing pump pulse duration (45 fs) and the dissociation time scales, theoretical interpretations of the experimental results most likely should consider the dressing of the potential energy surfaces by the laser field.[61]

The application of soft x-ray transient absorption spectroscopy is not confined to the study of strong-field physics. This technique is also harnessed to explore ultrafast dynamics initiated by photoexcitation in the weak-field, single-photon regime. For example, femtosecond time-resolved EXAFS spectroscopy has been reported at the Si $L_{2/3}$ ($2p$) edge with a HHG source.[62] The experimental data reveals a modulation of the Si—Si bond length following 800-nm excitation of a 100-nm-thick polycrystalline silicon thin foil. This modulation is attributed to the generation of coherent transverse acoustic and longitudinal optical phonons in the silicon sample by the NIR pump pulse. It is important to note that, in comparison to the measurements

done in Berkeley in which resonant near-edge transitions were probed, time-resolved EXAFS spectroscopy requires the HHG output to extend far beyond the absorption edge. For the Si $L_{2/3}$ edge located at 100 eV, x-ray photon energies of >0.5 keV are needed to allow accurate reconstruction of the contraction and expansion of the Si—Si bond. The production of high photon energies is achieved in this work by the use of a tight focusing geometry for HHG, resulting in peak intensities of $>10^{15}$ W/cm^2 for the driving laser in the HHG medium. The extension of this femtosecond EXAFS measurement technique to higher pump laser fluences will potentially reveal the breakdown of the crystalline lattice and the evolution of the density of states during the process of nonthermal melting, thereby bridging the information obtained from an earlier picosecond EXAFS work that elucidated the Si—Si bond lengths and the metallic nature of liquid silicon produced by nonthermal melting.[63]

Aside from soft x-ray pulses produced by HHG, femtosecond x-ray pulses that are produced by synchrotron-based pulse slicing schemes have also been successfully utilized in ultrafast x-ray absorption spectroscopy. Femtosecond x-ray absorption spectroscopy at a synchrotron facility was first used to investigate the optically induced insulator-to-metal transition in a thin VO_2 film.[64] Following photoexcitation by a NIR laser pulse, the dynamics of the phase transition are followed by monitoring the soft x-ray absorption at 516 eV and 540 eV as a function of pump-probe time delay; these photon energies originate from resonant transitions involving the V L_3 ($2p_{3/2}$) and O K ($1s$) absorption edges, respectively. Probing at these absorption edges allows the dynamics of valence band filling to be investigated, from which it is inferred that the insulator-to-metal transition is essentially complete after 3 ps.

In addition to probing element-specific dynamics in electronic materials, an exciting field to which synchrotron-produced femtosecond x-ray pulses has recently been applied is the study of ultrafast dynamics in magnetic materials.[65–67] Here, the ability of synchrotrons to generate elliptically polarized x-ray radiation presents a strong advantage over HHG; the latter produces linearly polarized light under normal circumstances, although the generation of elliptically polarized light by employing either phase-shifting mirrors[68] or aligned molecules as the HHG

target[69] has recently been reported. Elliptically polarized x-ray pulses are used to elucidate ultrafast magnetization dynamics via time-resolved x-ray magnetic circular dichroism (XMCD) spectroscopy. In these experiments, an optical pump pulse is used to induce demagnetization via the heating of electrons in the sample. Differential absorption spectra for x-ray probe pulses of opposite helicities are subsequently recorded as a function of pump-probe time delay. Performing XMCD at both spin-orbit split absorption features of a specific element, such as the L_2 and L_3 pre-edge resonances of Co, allows decomposition of the magnetization dynamics into contributions from spin and orbital angular momenta. Performing such an experiment on a $Co_{0.5}Pd_{0.5}$ thin film reveals distinct time scales for the thermalization of the spin and orbital angular momenta.[66]

A further advantage of performing time-resolved x-ray absorption measurements with pulse-sliced synchrotron radiation is the availability of higher x-ray photon energies for investigating ultrafast dynamics in solution. For example, the dynamics of spin cross-over in the transition metal complex $[Fe^{II}(bpy)_3]^{2+}$ has been investigated by probing at the Fe K (1*s*) edge with 250-fs time resolution.[70] It is found that the absorption signal at 7.126 keV increases as a function of pump-probe time delay with a time scale of 120 fs. This rise time is attributed to the formation of a metal-centered (ligand field) quintet state following the relaxation of the triplet metal-to-ligand charge-transfer (^{3}MLCT) state. The increase in absorption is consistent with the increase in the density of unoccupied states in the Fe 3*d* t_{2g} orbitals following spin cross-over. The measured time scale for this process is also in agreement with previous results obtained from femtosecond fluorescence upconversion and transient absorption spectroscopy in the optical domain.[71] In a different study, femtosecond x-ray absorption spectroscopy performed at the iodine L_1 and L_3 edges is used to investigate the ultrafast dynamics that accompany photoinduced charge-transfer-to-solvent in an aqueous iodide solution.[72] A broadening of the L_1 absorption resonance appears on the instrument response-limited time scale (250 fs) and is attributed to the formation of the transient $I(OH_2)$ species via hydrophobic solvation. This spectral signature, however, is absent from the picosecond x-ray transient absorption spectrum

collected at 50-ps time delay. Molecular dynamics simulations and quantum chemical calculations suggest that the $I(OH_2)$ species survives for 3 ps prior to solvation by the surrounding water molecules. Further extension of this work to measure femtosecond time-resolved EXAFS spectra offers a means of verifying this prediction.

The exciting possibility of resolving valence electron dynamics in real time lies beyond the broad range of ultrafast phenomena that are amenable to femtosecond core-level absorption spectroscopy. The exploration of this new frontier,[73–76] beyond the picosecond electron dynamics of Rydberg states,[77] requires much shorter pulse durations that are commensurate with the time scale of valence electronic motion. This is recently made possible by the advent of attosecond soft x-ray pulses.[29,78] Attosecond pulses are produced by driving HHG with carrier-envelope phase-stabilized, few-cycle laser pulses,[79] although variants that directly utilize the multi-cycle longer pulse output from an amplified Ti:sapphire laser system have also been demonstrated.[80] Attosecond time-resolved spectroscopy has been employed to investigate Auger decay in atoms,[30,81] the relative timing of electron photoemission from different states in a solid[82] and in an atomic gas,[83] and the manipulation of ionization[84] and dissociation[85] dynamics by laser fields. These experiments employ an attosecond soft x-ray pulse to initiate the electron dynamics, which is interrogated at a later time by the electric field of a few-cycle laser pulse. The rapid variation in the electric field strength of the laser pulse on a sub-half-cycle time scale modulates the energy of the primary or secondary electron released by the soft x-ray pump pulse, in analogy with the timed voltage sweep of a streak camera, from which attosecond dynamics can be reconstructed.[86] Alternatively, the confinement of tunnel ionization to a fraction of each half-cycle of the few-cycle laser field allows the high resolution probing of electron dynamics that occur near ionization thresholds.[81]

Attosecond soft x-ray transient absorption spectroscopy was recently introduced as an alternative approach to attosecond metrology.[87] It presents several complementary advantages over existing attosecond time-resolved pump-probe schemes. (1) Whereas the methods outlined above necessitate the ionization of the sample by the soft x-ray pulse in the pump step, transient

absorption spectroscopy provides access to the study of ultrafast dynamics in neutral, non-ionized species. (2) The ability of transient absorption to probe bulk samples complements the surface sensitivity of photoelectron spectroscopy. (3) Transient absorption probing can harness the entire spectral bandwidth that is associated with the attosecond temporal duration in order to achieve the optimal time resolution, while preserving high spectral resolution that is limited only by the linewidths of the probe transitions. In contrast, the spectral bandwidth of the attosecond pulses employed in photoelectron spectroscopy is constrained by the requirement to resolve adjacent photoelectron peaks, which limits the achievable time resolution. It is important to note that this particular advantage of attosecond transient absorption spectroscopy does not violate the time-energy uncertainty principle, since the spectral dispersion occurs only after the sample and is independent of the pump-probe cross-correlation.[88] The finite lifetime of the attosecond probe-induced polarization, however, implies that the transient absorption spectra acquired at a particular time delay encodes dynamics that occurs at all times after the pump-probe time delay until the polarization decays away.[89] This complication requires the use of numerical methods to retrieve quantitative information from the region of temporal overlap between the pump and probe pulses, during which the amplitude coefficients that are associated with the nonstationary state are still evolving with time. Fortunately this limitation can be overcome by judicious choice of a probe transition that has a short core-hole lifetime, such as the $M_{2/3}$ ($3p$) edges of first-row transition metals that are broadened by super-Coster-Krönig decay.[90] For example, the natural linewidth of the $M_{2/3}$ edge transition in Fe is ~5 eV,[91] which corresponds to a probe-induced polarization lifetime of only ~0.1 fs.

The recent extension of soft x-ray transient absorption spectroscopy into the attosecond time domain allowed the direct observation of valence electron motion accompanying the strong-field ionization of krypton atoms.[87] The creation of pairs of spin-orbit ground and excited states by strong-field ionization in previous work[42,44,92] begets the intriguing question as to whether electronic coherences exist in the resultant ion. A coherent superposition of the $^2P_{3/2}$ and $^2P_{1/2}$ spin-orbit states of Kr^+ would drive intra-atomic electron motion on the few-femtosecond time

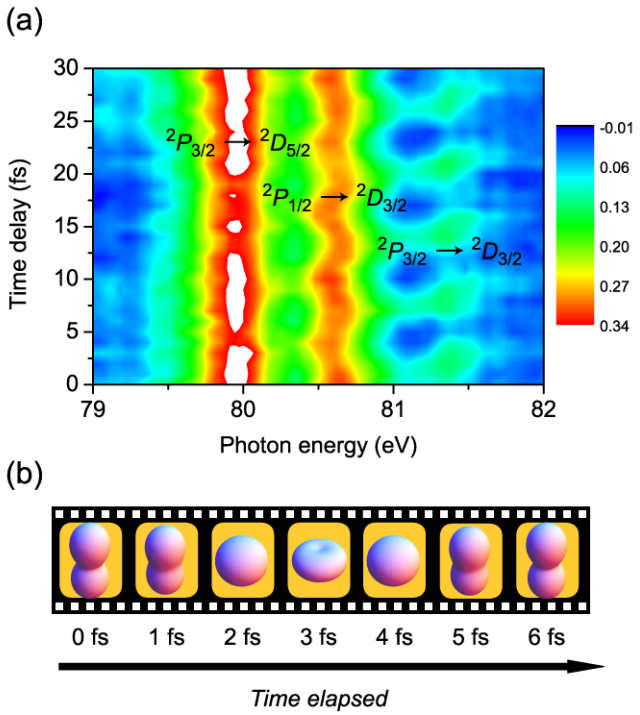

Figure 6. (a) Contour plot showing the soft x-ray transient absorption signal as a function of probe photon energy and time delay, following strong-field ionization of Kr atoms by an intense, sub-4-fs NIR laser pulse. The amplitude and energy modulations observed at the $^2P_{1/2} \rightarrow {}^2D_{3/2}$ and $^2P_{3/2} \rightarrow {}^2D_{3/2}$ transitions are spectroscopic signatures of electron motion. (b) Temporal evolution of the Kr^+ hole density, as reconstructed from the experimentally measured Kr^+ ion density matrix.

scale, as dictated by the relation $T = h/\Delta E_{SO}$, where T is the oscillation period, h is Planck's constant, and ΔE_{SO} is the spin-orbit splitting. While femtosecond time-resolved experiments have unambiguously revealed the creation of vibrational wave packets in small molecules by strong-field ionization,[93] the time-domain observation of electronic coherences produced by strong-field ionization requires attosecond temporal resolution. In the work reported in ref. 87, an intense, carrier-envelope phase-stabilized, sub-4-fs NIR pulse is used to strong-field-ionize a sample of Kr atoms, after which the electronic response of the Kr^+ ion is probed by a sub-150-as soft x-ray pulse centered at 80 eV.

The contour plot of the experimental data shows the transient absorption signal as a function of probe photon energy and pump-probe time delay (Figure 6). The observed probe

transitions at the Kr $M_{4/5}$ edge originate from the promotion of an electron from the 3*d* core level to the vacancy created by strong-field ionization in the 4*p* shell. The absorption lines for the $^2P_{1/2} \rightarrow {}^2D_{3/2}$ and $^2P_{3/2} \rightarrow {}^2D_{3/2}$ transitions exhibit both amplitude and energy modulations as a function of time. These modulations are spectroscopic signatures of electron motion that results from the coherent superposition of the Kr^+ $^2P_{3/2}$ and $^2P_{1/2}$ states. The creation of the spin-orbit wave packet can be rationalized by realizing that, in the presence of an intense laser field, the initial state produced by strong-field ionization is not diagonal in the $|j, m\rangle$ basis – in fact, due to the propensity for ionization to occur along the polarization axis of the strong-field ionization pulse, a p_z state is formed in the limit when the laser-atom interaction is much stronger than the spin-orbit splitting.[47] After the laser pulse, this field-dressed state evolves as a superposition of the $^2P_{3/2}$ and $^2P_{1/2}$ field-free eigenstates. The measured oscillation period of 6.3 ± 0.1 fs agrees with the period of 6.2 fs that is expected from the $^2P_{3/2}$ – $^2P_{1/2}$ spin-orbit splitting of 0.67 eV. The amplitude and energy modulations arise from the absorptive and dispersive components of the transient absorption signal, respectively.[94] In the spirit of our earlier work,[42] a global fit to the experimentally measured contour plot yields the quantum state distribution $\rho_{3/2,1/2}:\rho_{3/2,3/2}:\rho_{1/2,1/2} = 0.42 \pm 0.10 : 0.23 \pm 0.08 : 0.35 \pm 0.03$, where $\rho_{j,|m|}$ denotes the fraction of ions with total angular momentum *j* and projection quantum numbers $-m$ and $+m$. (Note that the cylindrical symmetry imposed by the linearly polarized strong-field ionization pulse requires $\rho_{j,-m} = \rho_{j,+m}$.) Together with the off-diagonal matrix element (see below), the time-dependent ion density matrix allows direct visualization of the motion of the hole in Kr^+ as a function of time. The theoretical quantum state distribution obtained by solving the time-dependent Schrödinger equation (TDSE) is $\rho_{3/2,1/2}:\rho_{3/2,3/2}:\rho_{1/2,1/2} = 0.69 : 0.05 : 0.26$. The origin of the discrepancy between the experimentally measured and theoretically calculated degree of alignment $\rho_{3/2,1/2}:\rho_{3/2,3/2}$ warrants further investigation. While the effect of the intense NIR pulse propagating through the sample will need to be examined more closely, a recent simulation showed that the propagation of the attosecond pulse through the sample target cannot account for this discrepancy.[89] It is interesting to note that a recent attosecond time-

resolved transient absorption measurement of Kr^+ ions created by strong-field ionization with monocycle NIR laser pulses (2.1 fs FWHM) yields $\rho_{3/2,1/2}:\rho_{3/2,3/2}:\rho_{1/2,1/2} = 0.400 \pm 0.024 : 0.315 \pm 0.024 : 0.285 \pm 0.004$,[95] which, compared to the work reported in ref. 87, seems to suggest that a shorter pulse duration leads to a lower degree of alignment for the Kr^+ $^2P_{3/2}$ state.

Beyond the ability to retrieve the relative populations of the different Kr^+ quantum states lies the unique capability of the attosecond soft x-ray transient absorption to measure the off-diagonal element (coherence term) of the Kr^+ ion density matrix. The measured relative amplitude of the off-diagonal element yields a degree of coherence $g = 0.63 \pm 0.17$ between the $^2P_{3/2}$ and $^2P_{1/2}$ states, in good agreement with $g = 0.65$ obtained from TDSE calculations. (In the limit of a coherent pure state, $g = 1$, whereas an incoherent statistical mixture yields $g = 0$. In recent improved experiments with a shorter pump pulse,[95] $g = 0.85$) In general, the mismatch between the periodicity of ionization (1.25 fs for a carrier wavelength of 750 nm) and the periodicity of the Kr^+ spin-orbit wave packet (6.2 fs) would negate any coherence that survives beyond the laser pulse when a long multi-cycle ionization pulse is used.[96] In this study, the non-vanishing coherence is due to the use of a few-cycle pulse for strong-field ionization. This result not only demonstrates the feasibility of performing transient absorption spectroscopy with attosecond time resolution, it also points to the possibility of employing strong-field ionization as a general strategy for initiating nonstationary electron dynamics.

Aside from observing coherent electron motion, attosecond time-resolved transient absorption spectroscopy can also be applied to investigate the autoionization dynamics of highly excited states.[97] This work extends into the time domain the earlier work on the laser dressing of He double excitation states.[49] In ref. 97, an isolated attosecond pulse with spectrum spanning 20 – 40 eV is used to excite the 3*s* inner-valence electron of Ar. The resultant $3s3p^6np$ ($n = 4 – 6$) excited states decay by autoionization to the Ar^+ $3s^23p^5\varepsilon l$ continuum. In the presence of a moderately intense NIR laser pulse ($I_0 \sim 5 \times 10^{11}$ W/cm^2), the decay of these autoionizing states is disrupted by laser-induced coupling either to the continuum or to neighboring autoionizing states. The former maps out the population decay of the autoionizing state as the soft x-ray-NIR

time delay is scanned, hence allowing autoionization lifetimes to be measured directly in the time domain. For the $3s3p^6 4p$ and $3s3p^6 5p$ states, the experimental results suggest autoionization lifetimes that are in agreement with those inferred from the natural linewidths of their resonances. However careful attention must be paid to the appropriate choice of the probe photon energy and spectral resolution in these lifetime measurements, since coupling to adjacent autoionizing states could present potential complications. Indeed, the development of the $3s3p^6 4p$ peak into an Autler-Townes doublet is observed in the vicinity of zero time delay due to coupling to the $3s3p^6 4d$ state. Ideally, global analysis of the experimental data should be performed to yield quantitative information on the coupling of an autoionizing state to other states and to the continuum.

The attosecond time-resolved experiments described insofar consider only the envelope of the HHG-produced soft x-ray pulse. In reality, the periodicity of the HHG process when driven by a multi-cycle laser field results in a train of attosecond pulses. Attosecond pulse trains, by virtue of their periodicity in time, are ideal for studying strong-field processes via wave packet interferometry.[98] Attosecond pulse trains can also be employed in transient absorption measurements in which the pump-probe time delay is varied with attosecond, sub-laser-cycle precision. Recently this technique was used to address the origin of the observed modulation of the He^+ ion yield[99] on the sub-cycle time scale when a He gas target is simultaneously irradiated by a soft x-ray attosecond pulse train and a weak NIR field derived from the HHG driving laser.[100] It is found that the intensities of the 13th and the 15th harmonics oscillate as a function of time delay between the soft x-ray and NIR pulses with a periodicity that corresponds to half the period of the NIR laser cycle ($T_L/2 = 1.33$ fs for an 800 nm laser field). Furthermore the relative phase at which the two harmonics oscillate varies with the peak intensity of the fundamental laser field. It should be noted that the photon energies of these harmonics – 20.5 eV for the 13th harmonic and 23.7 eV for the 15th harmonic – are below the ionization threshold of He. Therefore any observed dynamics must involve the field-dressed He $1snp$ Rydberg states. The experimental result can be understood in terms of wave packet interferometry: an electron wave

packet created below the ionization threshold by a given pulse in the attosecond pulse train is launched into the continuum by the NIR laser field and, upon its return to the ion core, interferes with an electron wave packet launched by the following pulse in the pulse train. Within this framework, the observed laser intensity-dependent phase shift can be attributed to the modification of the excursion time of the electron wave packet in the continuum by the NIR laser intensity. Thus, compared to the ion yield measurement, which probes the effect of wave packet interference on the integrated ionization cross-section of the He atom, this spectrally-resolved transient absorption study provides complementary information regarding the phase shifts of the different He bound state absorption channels.

Looking to the future, soft x-ray transient absorption spectroscopy is expected to find widespread applicability to the study of ultrafast quantum dynamics, particularly when performed with attosecond time resolution. The electron dynamics that can be interrogated by this new technique are not limited to those that accompany strong-field ionization. The emergence of sub-femtosecond pulses in the deep ultraviolet[101] as a single-photon excitation light source will allow coherent electron-nuclear dynamics that accompany photochemical and/or photophysical transformations to be probed with attosecond time resolution.[102] In addition, attosecond transient absorption can be used to investigate the manipulation of electron dynamics on the sub-cycle time scale by optical pulses.[103,104] The availability of higher x-ray photon energies and larger spectral bandwidths – the production of photons up to 3.5 keV and with bandwidths of ~0.6 keV from femtosecond HHG sources have already been demonstrated[105,106] – will allow attosecond EXAFS spectroscopy to directly resolve some of the most rapid molecular dynamics, such as the isomerization of the CH_4^+ ion that is suggested to occur on sub-femtosecond time scales.[107] Although the application of HHG-produced keV x-rays to static EXAFS spectroscopy is already successful,[105] progress towards time-resolved EXAFS in the keV requires a boost in photon flux in this energy range, which by itself is an area of active research.[108,109] Finally, the implementation of novel schemes for generating high-energy attosecond pulses at x-ray free-electron lasers[110] will enable true attosecond x-ray pump-

attosecond x-ray probe transient absorption experiments, currently beyond reach due to the low photon flux of attosecond tabletop HHG sources. Such experiments promise access to the holy grail of attosecond science – the ability to observe correlated electron dynamics in real time.[111,112]

Acknowledgements

Our work on soft x-ray transient absorption spectroscopy has benefitted immensely from discussions with M. Khalil, T. Pfeifer, R. Santra, C. H. Greene, M. M. Murnane, H. C. Kapteyn, E. Goulielmakis and F. Krausz. We are grateful for support from the LDRD program at LBNL, the National Science Foundation (EEC-0310717 and CHE-1049946), the Air Force Office of Scientific Research (FA9550-04-1-0242), the W. M. Keck Foundation, the Department of Defense National Security Science and Engineering Faculty Fellowship, and the Director, Office of Science, Office of Basic Energy Sciences, US Department of Energy (DE-AC02-05-CH11231).

Biographies

Zhi-Heng Loh performed both his graduate and postdoctoral work under the mentorship of Professor Stephen Leone at the University of California, Berkeley. He joined Nanyang Technological University as an Assistant Professor in December 2010. Website: http://www.spms.ntu.edu.sg/cbc/FacultyResearch/Individual%20Faculty/ZHLoh.html

Stephen R. Leone is a Professor of Chemistry and Physics at the University of California at Berkeley and Director of the Chemical Dynamics Beamline, Lawrence Berkeley National Laboratory. Recent honors include the American Chemical Society Peter Debye Award (2005) and the American Physical Society Irving Langmuir Prize in Chemical Physics (2011). Website: http://www.cchem.berkeley.edu/leonegrp/

References

(1) Norrish, R. G. W.; Porter, G. Chemical Reactions Produced by Very High Light Intensities. *Nature* **1949**, *164*, 658–658.

(2) Zewail, A. H. Femtochemistry: Atomic-Scale Dynamics of the Chemical Bond *J. Phys. Chem. A* **2000**, *104*, 5660–5694.

(3) Polli, D.; Lüer, L.; Cerullo, G. High-Time-Resolution Pump-Probe System with Broadband Detection for the Study of Time-Domain Vibrational Dynamics. *Rev. Sci. Instrum.* **2007**, *78*, 103108-1–103108-9.

(4) Schriever, C.; Lochbrunner, S.; Riedle, E.; Nesbitt, D. J.; Ultrasensitive Ultraviolet-Visible 20 fs Absorption Spectroscopy of Low Vapor Pressure Molecules in the Gas Phase. *Rev. Sci. Instrum.* **2008**, *79*, 013107-1–013107-9.

(5) Megerle, U.; Pugliesi, I.; Schriever, C.; Sailer, C. F.; Riedle, E.; Sub-50 fs Broadband Absorption Spectroscopy with Tunable Excitation: Putting the Analysis of Ultrafast Molecular Dynamics on Solid Ground. *Appl. Phys. B* **2009**, *96*, 215–231.

(6) Beard, M. C.; Turner, G. M.; Schmuttenmaer, C. A. Transient Photoconductivity in GaAs as Measured by Time-Resolved Terahertz Spectroscopy. *Phys. Rev. B* **2000**, *62*, 15764–15777.

(7) Chen, L. X.; Jäger, W. J. H.; Jennings, G.; Gosztola, D. J.; Munkholm, A.; Hessler, J. P. Capturing a Photoexcited Molecular Structure Through Time-Domain X-Ray Absorption Fine Structure. *Science* **2001**, *292*, 262–264.

(8) Fork, R. L.; Brito-Cruz, C. H.; Becker, P. C.; Shank, C. V. Compression of Optical Pulses to Six Femtoseconds by Using Cubic Phase Compensation. *Opt. Lett.* **1987**, *12*, 483–485.

(9) Brabec, T.; Krausz, F. Intense Few-Cycle Laser Fields: Frontiers of Nonlinear Optics. *Rev. Mod. Phys.* **2000**, *72*, 545–591.

(10) Shirakawa, A.; Sakane, I.; Takasaka, M.; Kobayashi, T. Sub-5-fs Visible Pulse Generation by Pulse-Front-Matched Noncollinear Optical Parametric Amplification *Appl. Phys. Lett.* **1999**, 74, 2268 – 2270.

(11) Kobayashi, T.; Saito, T.; Ohtani, H. Real-Time Spectroscopy of Transition States in Bacteriorhodopsin during Retinal Isomerization. *Nature* **2001**, *414*, 531–534.

(12) Stohr, J. *NEXAFS Spectroscopy (Springer Series in Surface Sciences)*, Springer: New York, **2003**.

(13) Bressler. C; Chergui, M. Molecular Structural Dynamics Probed by Ultrafast X-Ray Absorption Spectroscopy. *Annu. Rev. Phys. Chem.* **2010**, *61*, 263–282.

(14) Chen, L.X. Probing Transient Molecular Structures in Photochemical Processes Using Laser-Initiated Time-Resolved X-Ray Absorption Spectroscopy. *Annu. Rev. Phys. Chem.* **2005**, *56*, 221–254.

(15) Ráksi, F.; Wilson, K. R.; Jiang, Z.; Ikhlef, A.; Côté, C. Y.; Kieffer, J.-C. Ultrafast X-Ray Absorption Probing of a Chemical Reaction. *J. Chem. Phys*. **1996**, *104*, 6066–6069.

(16) Lee, T.; Jiang, Y.; Rose-Petruck, C. G.; Benesch, F. Ultrafast Tabletop Laser-Pump–X-Ray Probe Measurement of Solvated $Fe(CN)_6^{4-}$. *J. Chem. Phys*. **2005**, *122*, 084506-1–084506-8.

(17) Schoenlein, R. W.; Chattopadhyay, S.; Chong, H. H. W.; Glover, T. E.; Heimann, P. A.; Shank, C. V.; Zholents, A. A.; Zolotorev, M. S. Generation of Femtosecond Pulses of Synchrotron Radiation. *Science* **2000**, *287*, 2237–2240.

(18) Ackermann, W.; Asova, G.; Ayvazyan, V.; Azima, A.; Baboi, N.; Bähr, H.; Balandin, V.; Beutner, B.; Brandt, A.; Bolzmann, A., *et al*. Operation of a Free-Electron Laser from the Extreme Ultraviolet to the Water Window. *Nature Photon.* **2007**, *1*, 336–342.

(19) Emma, P.; Akre, A.; Arthur, J.; Bionta, R.; Costedt, C.; Bozek, J.; Brachmann, A.; Bucksbaum, P.; Coffee, R.; Decker, F.-J.; *et al*. First Lasing and Operation of an Angstrom-Wavelength Free-Electron Laser. *Nature Photon.* **2010**, *4*, 641–647.

(20) Ding, Y.; Brachmann, A.; Decker, F.-J.; Dowell, D.; Emma, P.; Frisch, J.; Gilevich, S.; Hays, G.; Hering, Ph.; Huang, Z.; Iverson, R.; Loos, H.; Miahnahri, A.; Nuhn, H.-D.; Ratner, D.; Turner, J.; Welch, J.; White, W.; Wu, J. Measurements and Simulations of Ultralow Emittance and Ultrashort Electron Beams in the Linac Coherent Light Source. *Phys. Rev. Lett*. **2009**, *102*, 254801-1–254801-4.

(21) Murnane, M. M.; Kapteyn, H. C.; Falcone, R. W. Generation of Efficient Ultrafast Laser-Plasma X-Ray Sources. *Phys. Fluids B* **1991**, *3*, 2409–2413.

(22) Kieffer, J. C.; Chaker, M.; Matte, J. P.; Pépin, H.; Côté, C. Y.; Beaudoin, Y.; Johnston T. W.; Chien, C. Y.; Coe, S.; Mourou, G.; Peyrusse, O. Ultrafast X-Ray Sources. *Phys. Fluids B* **1993**, *5*, 2676–2681.

(23) Popmintchev, T.; Chen, M.-C.; Arpin, P.; Murnane, M. M.; Kapteyn, H. C. The Attosecond Nonlinear Optics of Bright Coherent X-Ray Generation. *Nature Photon.* **2010**, *4*, 822–832.

(24) Antoine, P.; L'Huillier, A.; Lewenstein, M. Attosecond Pulse Trains Using High-Order Harmonics. *Phys. Rev. Lett.* **1996**, *77*, 1234–1237.

(25) Poletto, L.; Villoresi, P.; Benedetti, E.; Ferrari, F.; Stagira, S.; Sansone, G.; Nisoli, M. Intense Femtosecond Extreme Ultraviolet Pulses by Using a Time-Delay-Compensated Monochromator. *Opt. Lett.* **2007**, *32*, 2897–2899.

(26) Nugent-Glandorf, L.; Scheer, M.; Samuels, D. A.; Mulhisen, A. M.; Grant, E. R.; Yang, X.; Bierbaum, V. M.; Leone, S. R. Ultrafast Time-Resolved Soft X-Ray Photoelectron Spectroscopy of Dissociated Br_2. *Phys. Rev. Lett.* **2001**, *87*, 193002-1–193002-4.

(27) Bauer, M.; Lei, C.; Read, K.; Tobey, R.; Gland, J.; Murnane, M. M.; Kapteyn, H. C. Direct Observation of Surface Chemistry Using Ultrafast Soft-X-Ray Pulses. *Phys. Rev. Lett.* **2001**, *87*, 025501-1–025501-4.

(28) Siffalovic, P.; Drescher, M.; Spieweck, M.; Wiesenthal, T.; Lim, Y. C.; Weidner, R.; Elizarov, A.; Heinzmann, U. Laser-Based Apparatus for Extended Ultraviolet Femtosecond Time-Resolved Photoemission Spectroscopy. *Rev. Sci. Instrum.* **2001**, *72*, 30–35.

(29) Hentschel, M.; Kienberger, R.; Spielmann, C.; Reider, G. A.; Milosevic, N.; Brabec, T.; Corkum, P.; Heinzmann, U.; Drescher, M.; Krausz, F. Attosecond Metrology. *Nature* **2001**, *414*, 509–513.

(30) Drescher, M.; Hentschel, M.; Kienberger, R.; Uiberacker, M.; Yakovlev, V.; Scrinz, A.; Westerwalbesloh, T.; Kleineberg, U.; Heinzmann, U.; Krausz, F. Time-Resolved Atomic Inner-Shell Spectroscopy. *Nature* **2002**, *419*, 803–807.

(31) Takahashi, E.; Nabekawa, Y.; Otsuka, T.; Obara, M.; Midorikawa, K. Generation of Highly Coherent Submicrojoule Soft X Rays by High-Order Harmonics. *Phys. Rev. A* **2002**, *66*, 021802-1–021802-4.

(32) Yost, D. C.; Cingöz, A.; Allison, T. K.; Ruehl, A.; Fermann, M. E.; Hartl, I.; Ye, J. Power optimization of XUV frequency combs for spectroscopy applications. *Opt. Express* **2011**, *19*, 23483–23493.

(33) Huse, N.; Wen, H.; Nordlund, D.; Szilagyi, E.; Daranciang, D.; Miller, T. A.; Nilsson, A.; Schoenlein, R. W.; Lindenberg, A. M. Probing the hydrogen-bond network of water via time-resolved soft x-ray spectroscopy. *Phys. Chem. Chem. Phys*. **2009**, *11*, 3951–3957.

(34) Benesch, F.; Lee, T.; Jiang, Y.; Rose-Petruck, C. G. Ultrafast Laser-Driven X-Ray Spectrometer for X-Ray Absorption Spectroscopy of Transition Metal Complexes *Opt. Lett*. **2004**, *29*, 1028–1030.

(35) Khan, S.; Holldack, K.; Kachel, T.; Mitzner, R.; Quast, T. Femtosecond Undulator Radiation from Sliced Electron Bunches. *Phys. Rev. Lett*. **2006**, *97*, 074801-1–074801-4.

(36) Tavella, F.; Stojanovic, N.; Geloni, G.; Gensch, M. Few-Femtosecond Timing at Fourth-Generation X-Ray Light Sources. *Nature Photon.* **2011**, *5*, 162–165.

(37) Oguri, K.; Nishikawa, T.; Ozaki, T.; Nakano, H. Sampling Measurement of Soft-X-Ray-Pulse Shapes by Femtosecond Sequential Ionization of Kr^+ in an Intense Laser Field. *Opt. Lett*. **2004**, *29*, 1279–1281.

(38) Oguri, K.; Nakano, H.; Nishikawa, T.; Uesugi, N. Cross-Correlation Measurement of Ultrashort Soft X-Ray Pulse Emitted from Femtosecond Laser-Produced Plasma Using Optical Field-Induced Ionization. *Appl. Phys. Lett*. **2001**, *79*, 4506–4508.

(39) Krässig, B.; Dunford, R. W.; Kanter, E. P.; Landahl, E. C.; Southworth, S. H.; Young, L. A Simple Cross-Correlation Technique between Infrared and Hard X-Ray Pulses. *Appl. Phys. Lett*. **2009**, *94*, 171113-1–171113-3.

(40) Protopapas, M.; Keitel, C. H.; Knight, P. L. Atomic Physics with Super-High Intensity Lasers. *Rep. Prog. Phys.* **1997**, *60*, 389–486.

(41) Loh, Z.-H.; Khalil, M.; Correa, R. E.; Leone, S. R. A tabletop femtosecond time-resolved soft x-ray transient absorption spectrometer. *Rev. Sci. Instrum*. **2008**, *79*, 073101-1–073101-13.

(42) Loh, Z.-H.; Khalil, M.; Correa, R. E.; Santra, R.; Buth, C.; Leone, S. R. Quantum State-Resolved Probing of Strong-Field-Ionized Xenon Atoms using Femtosecond High-Order Harmonic Transient Absorption Spectroscopy. *Phys. Rev. Lett.* **2007**, *98*, 143601-1–143601-4.

(43) Gubbini, E.; Eichmann, U.; Kalashnikov, M.; Sandner, W. Core Relaxation in Atomic Ultrastrong Laser Field Ionization. *Phys. Rev. Lett.* **2005**, *94*, 053602-1–053602-4.

(44) Young, L.; Arms, D. A.; Dufresne, E. M.; Dunford, R. W.; Ederer, D. L.; Höhr, C.; Kanter, E. P.; Krässig, B.; Landahl, E. C.; Peterson, E. R.; Rudati, J.; Santra, R.; Southworth, S. H. X-Ray Microprobe of Orbital Alignment in Strong-Field Ionized Atoms. *Phys. Rev. Lett.* **2006**, *97*, 083601-1–083601-4.

(45) Lin, M. F.; Pfeiffer, A. N.; Neumark, D. M.; Leone, S. R.; Gessner, O. Strong-Field Induced XUV Transmission and Multiplet Splitting in $4d^{-1}6p$ Core-excited Xe studied by Femtosecond XUV Transient Absorption Spectroscopy. *J. Chem. Phys*., in press.

(46) Southworth, S. H.; Arms, D. A.; Dufresne, E. M.; Dunford, R. W.; Ederer, D. L.; Höhr, C.; Kanter, E. P.; Krässig, B.; Landahl, E. C.; Peterson, E. R.; Rudati, J.; Santra, R.; Walko, D. A.; Young, L. K-Edge X-Ray Absorption Spectroscopy of Laser-Generated Kr^+ and Kr^{2+}. *Phys. Rev. A* **2007**, *76*, 043421-1–043421-9.

(47) Santra, R.; Dunford, R. W.; Young, L. Spin-Orbit Effect on Strong-Field Ionization of Krypton. *Phys. Rev. A* **2006**, *74*, 043403-1–043403-9.

(48) Mevel, E.; Breger, P.; Trainham, R.; Petite, G.; Agostini, P.; Migus, A.; Chambaret, J.-P.; Antonetti, A. Atoms in Strong Optical Fields: Evolution from Multiphoton to Tunnel Ionization. *Phys. Rev. Lett.* **1993**, *70*, 406–409.

(49) Loh, Z.-H.; Greene, C. H.; Leone, S. R. Femtosecond Induced Transparency and Absorption in the Extreme Ultraviolet by Coherent Coupling of the He $2s2p$ ($^1P^o$) and $2p^2$ ($^1S^e$) Double Excitation States with 800 nm Light. *Chem. Phys.* **2008**, *350*, 7–13.

(50) Fleischhauer, M.; Imamoglu, A.; Marangos, J. P. Electromagnetically Induced Transparency: Optics in Coherent Media. *Rev. Mod. Phys*. **2005**, *77*, 633–673.

(51) Buth, C.; Santra, R.; Young, L. Electromagnetically Induced Transparency for X-Rays. *Phys. Rev. Lett*. **2007**, *98*, 253001-1–253001-4.

(52) Fano, U. Effects of Configuration Interaction on Intensities and Phase Shifts. *Phys. Rev.* **1961**, *124*, 1866–1878.

(53) Madden, R. P.; Codling, K. New Autoionizing Atomic Energy Levels in He, Ne, and Ar. *Phys. Rev. Lett.* **1963**, *10*, 516–518.

(54) Glover, T. E.; Hertlein, M. P.; Southworth, S. H.; Allison, T. K.; van Tilborg, J.; Kanter, E. P.; Krässig, B.; Varma, H. R.; Rude, B.; Santra, R.; Belkacem, A.; Young, L. Controlling X-Rays with Light. *Nature Phys.* **2009**, *6*, 69–74.

(55) Pfeiffer, A. N.; Leone, S. R. Transmission of an Isolated Attosecond Pulse in a Strong-Field Dressed Atom. *Phys. Rev. A* **2012**, *85*, 053422-1–053422-6.

(56) Loh, Z.-H.; Leone, S. R. Ultrafast Strong-Field Dissociative Ionization Dynamics of CH_2Br_2 Probed by Femtosecond Soft X-Ray Transient Absorption Spectroscopy. *J. Chem. Phys.* **2008**, *128*, 204302-1–204302-8.

(57) Levis, R. J.; Menkir, G. M.; Rabitz, H. Selective Bond Dissociation and Rearrangement with Optimally Tailored, Strong-Field Laser Pulses. *Science* **2001**, *292*, 709–713.

(58) Sussman, B. J.; Townsend, D.; Ivanov, M. Yu.; Stolow, A. Dynamic Stark Control of Photochemical Processes. *Science* **2006**, *314*, 278–281.

(59) Hankin, S. M.; Villeneuve, D. M.; Corkum, P. B.; Rayner, D. M. Intense-Field Laser Ionization Rates in Atoms and Molecules. *Phys. Rev. A* **2001**, *64*, 013405-1–013405-12.

(60) Huang, J.; Xu, D.; Fink, W. H.; Jackson, W. M. Photodissociation of the Dibromomethane Cation at 355 nm by means of Ion Velocity Imaging. *J. Chem. Phys*. **2001**, *115*, 6012–6017.

(61) Posthumus, J. H. The Dynamics of Small Molecules in Intense Laser Fields. *Rep. Prog. Phys.* **2004**, *67*, 623–665.

(62) Seres, E.; Spielmann, C. Ultrafast Soft X-Ray Absorption Spectroscopy with Sub-20-fs Resolution. *Appl. Phys. Lett.* **2007**, *91*, 121919-1 –121919-3.

(63) Johnson, S. L.; Heimann, P. A.; Lindenberg, A. M.; Jeschke, H. O.; Garcia, M. E.; Chang, Z.; Lee, R. W.; Rehr, J. J.; Falcone, R. W. Properties of Liquid Silicon Observed by

Time-Resolved X-Ray Absorption Spectroscopy. *Phys. Rev. Lett*. **2003**, *91*, 157403-1–157403-4.

(64) Cavalleri, A.; Rini, M.; Chong, H. H. W.; Fourmaux, S.; Glover, T. E.; Heimann, P. A.; Kieffer, J. C.; Schoenlein, R. W. Band-Selective Measurements of Electron Dynamics in VO_2 Using Femtosecond Near-Edge X-Ray Absorption. *Phys. Rev. Lett.* **2005**, *95*, 067405-1–067405-4.

(65) Beaurepaire, E.; Merle, J.-C.; Daunois, A.; Bigot, J.-Y. Ultrafast Spin Dynamics in Ferromagnetic Nickel. *Phys. Rev. Lett*. **1996**, *76*, 4250–4253.

(66) Boeglin, C.; Beaurepaire, E.; Halté, V.; López-Flores, V.; Stamm, C.; Pontius, N.; Dürr, H. A.; Bigot, J.-Y. Distinguishing the Ultrafast Dynamics of Spin and Orbital Moments in Solids. *Nature* **2010**, *465*, 458–461.

(67) Wietstruk, M.; Melnikov, A.; Stamm, C.; Kachel, T.; Pontius, N.; Sultan, M.; Gahl, C.; Weinelt, M.; Dürr, H. A.; Bovensiepen, U. Hot-Electron-Drive Enhancement of Spin-Lattice Coupling in Gd and Tb 4*f* Ferromagnets Observed by Femtosecond X-Ray Magnetic Circular Dichroism. *Phys. Rev. Lett.* **2011**, *106*, 127401-1–127401-4.

(68) Vodungbo, B.; Sardinha, A. B.; Gautier, J.; Lambert, G.; Valentin, C.; Lozano, M.; Iaquaniello, G.; Delmotte, F.; Sebban, S.; Lüning, J.; Zeitoun, P. Polarization Control of High Order Harmonics in the EUV Photon Energy Range. *Opt. Express* **2011**, *19*, 4346–4356.

(69) Zhou, X.; Lock, R.; Wagner, N.; Li, W.; Kapteyn, H. C.; Murnane, M. M. Elliptically Polarized High-Order Harmonic Emission from Molecules in Linearly Polarized Laser Fields. *Phys. Rev. Lett*. **2009**, *102*, 073902-1–073902-4.

(70) Bressler, Ch.; Milne, C.; Pham, V.-T.; ElNahhas, A.; van der Veen, R. M.; Gawelda, W.; Johnson, S.; Beaud, P.; Grolimund, D.; Kaiser, M.; Borca, C. N.; Ingold, G.; Abela, R.;

Chergui, M. Femtosecond XANES Study of the Light-Induced Spin Crossover Dynamics in an Iron(II) Complex. *Science* **2009**, *323*, 489–492.

(71) Gawelda, W.; Cannizzo, A.; Pham, V.-T.; van Mourik, F.; Bressler, C.; Chergui, M. Ultrafast Nonadiabatic Dynamics of $[Fe^{II}(bpy)_3]^{2+}$ in Solution. *J. Am. Chem. Soc*. **2007**, *129*, 8199–8206.

(72) Pham, V.-T.; Penfold, T. J.; van der Veen, R. M.; Lima, F.; El Nahhas, A.; Johnson, S. L.; Beaud, P.; Abela, R.; Bressler, C.; Tavernelli, I.; Milne, C. J.; Chergui, M. Probing the Transition from Hydrophilic to Hydrophobic Solvation with Atomic Scale Resolution. *J. Am. Chem. Soc*. **2011**, *133*, 12740–12748.

(73) Pfeifer, T.; Abel, M. J.; Nagel, P. M.; Jullien, A.; Loh, Z.-H.; Bell, M. J.; Neumark, D. M.; Leone, S. R. Time-Resolved Spectroscopy of Attosecond Quantum Dynamics. *Chem. Phys. Lett*. **2008**, *463*, 11–24.

(74) Krausz, F.; Ivanov, M. Attosecond Physics. *Rev. Mod. Phys.* **2009**, *81*, 163–234.

(75) Kling, M. F.; Vrakking, M. J. J. Attosecond Electron Dynamics. *Annu. Rev. Phys. Chem*. **2008**, *59*, 463–492.

(76) Gallmann, L.; Cirelli, C.; Keller, U. Attosecond Science: Recent Highlights and Future Trends. *Annu. Rev. Phys. Chem*. **2012**, *63*, 447–469.

(77) Jones, R. R.; Noordam, L. D. Electronic Wavepackets. *Adv. Atom Mol. Opt. Phys*. **1997**, *38*, 1–38.

(78) Fieß, M.; Schultze, M.; Goulielmakis, E.; Dennhardt, B; Gagnon, J.; Hofstetter, M.; Kienberger, R.; Krausz, F. Versatile Apparatus for Attosecond Metrology and Spectroscopy. *Rev. Sci. Instrum*. **2010**, *81*, 093103-1–093103-8.

(79) Baltuška, A.; Udem, T.; Uiberacker, M.; Hentschel, M.; Goulielmakis, E.; Gohle, C.; Holzwarth, R.; Yakovlev, V. S.; Scrinzi, A.; Hänsch, T. W.; Krausz, F. Attosecond Control of Electronic Processes by Intense Light Fields. *Nature* **2003**, *421*, 611–615.

(80) Gilbertson, S.; Khan, S. D.; Wu, Y.; Chini, M.; Chang, Z. Isolated Attosecond Pulse Generation Without the Need to Stabilize the Carrier-Envelope Phase of Driving Lasers. *Phys. Rev. Lett.* **2010**, *105*, 093902-1–093902-4.

(81) Uiberacker, M.; Uphues, T.; Schultze, M.; Verhoef, A. J.; Yakovlev, V.; Kling, M. F.; Rauschenberger, J.; Kabachnik, N. M.; Schröder, H.; Lezius, M.; Kompa, K. L.; Muller, H.-G.; Vrakking, M. J. J.; Hendel, S.; Kleineberg, U.; Heinzmann, U.; Drescher, M.; Krausz, F. Attosecond Real-Time Observation of Electron Tunnelling in Atoms. *Nature* **2007**, *446*, 627–632.

(82) Cavalieri, A. L.; Muller, N.; Uphues, T.; Yakovlev, V. S.; Baltuška, A.; Horvath, B.; Schmidt, B.; Blumel, L.; Holzwarth, R.; Hendel, S.; Drescher, M.; Kleineberg, U.; Echenique, P. M.; Kienberger, R.; Krausz, F.; Heinzmann, U. Attosecond Spectroscopy in Condensed Matter. *Nature* **2007**, *449*, 1029–1032.

(83) Schultze, M.; Fieß, M.; Karpowicz, N.; Gagnon, J.; Korbman, M.; Hofstetter, M.; Neppl, S.; Cavalieri, A. L.; Komninos, Y.; Mercouris, T.; Nicolaides, C. A.; Pazourek, R.; Nagele, S.; Feist, J.; Burgdöfer, J.; Azzeer, A. M.; Ernstorfer, R.; Kienberger, R.; Kleineberg, U.; Goulielmakis, E.; Krausz, F.; Yakovlev, V. S. Delay in Photoemission. *Science* **2010**, *328*, 1658–1662.

(84) Gilbertson, S.; Chini, M.; Feng, X.; Khan, S.; Wu, Y.; Chang, Z. Monitoring and Controlling the Electron Dynamics in Helium with Isolated Attosecond Pulses. *Phys. Rev. Lett.* **2010**, *105*, 263003-1–263003-4.

(85) Sansone, G.; Kelkensberg, F.; Perez-Torres, J. F.; Morales, F.; Kling, M. F.; Siu, W.; Ghafur, O.; Johnsson, P.; Swoboda, M.; Benefetti, E.; Ferrari, F.; Lepine, F.; Sanz-Vicario, J. L.; Zherebtsov, S.; Znakovskaya, I.; L'Huiller, A.; Ivanov, M. Y.; Nisoli, M.; Martin, F.; Vrakking, M. J. J. Electron Localization Following Attosecond Molecular Photoionization. *Nature* **2010**, *465*, 763–766.

(86) Itatani, J.; Quéré, F.; Yudin, G. L.; Ivanov, M. Yu.; Krausz, F.; Corkum, P. B. Attosecond Streak Camera. *Phys. Rev. Lett.* **2002**, *88*, 173903-1–173903-4.

(87) Goulielmakis, E.; Loh, Z.-H.; Wirth, A.; Santra, R.; Rohringer, N.; Yakovlev, V. S.; Zherebtsov, S.; Pfeifer, T.; Azzeer, A. M.; Kling, M. F.; Leone, S. R.; Krausz, F. Real-Time Observation of Valence Electron Motion. *Nature* **2010**, *466*, 739–743.

(88) Pollard, W. T.; Mathies, R. A. Analysis of Femtosecond Dynamic Absorption Spectra of Nonstationary States. *Annu. Rev. Phys. Chem.* **1992**, *43*, 497–523.

(89) Santra, R.; Yakovlev, V. S.; Pfeifer, T.; Loh, Z.-H. Theory of Attosecond Transient Absorption Spectroscopy of Strong-Field-Generated Ions. *Phys. Rev. A* **2011**, *83*, 033405-1–033405-9.

(90) Davis, L. C.; Feldkamp, L. A. Resonant Photoemission Involving Super-Coster-Kronig Transitions. *Phys. Rev. B* **1981**, *23*, 6239–6253.

(91) Bruhn, R.; Sonntag, B.; Wolff, H. W. 3*p* Excitations of Atomic and Metallic Fe, Co, Ni and Cu. *J. Phys. B* **1979**, *12*, 203–212.

(92) Rottke, H.; Ludwig, J.; Sandner, W. 'Short' Pulse MPI of Xenon: The $^2P_{1/2}$ Ionization Channel. *J. Phys. B* **1996**, *29*, 1479–1487.

(93) Ergler, Th.; Rudenko, A.; Feuerstein, B.; Zrost, K.; Schröter, C. D.; Moshammer, R.; Ullrich, J. Spatiotemporal Imaging of Ultrafast Molecular Motion: Collapse and Revival of the D_2^+ Nuclear Wave Packet. *Phys. Rev. Lett.* **2006**, *97*, 193001-1–193001-4.

(94) Pollard, W. T.; Lee, S.-Y.; Mathies, R. A.; Wave Packet Theory of Dynamics Absorption Spectra in Femtosecond Pump-Probe Experiments. *J. Chem. Phys.* **1990**, *92*, 4012–4029.

(95) Wirth, A.; Hassan, M. Th.; Grguras, I.; Gagnon, J.; Moulet, A.; Luu, T. T.; Pabst, S.; Santra, R.; Alahmed, Z. A.; Azzeer, A. M.; Yakovlev, V. S.; Pervak, V.; Krausz, F.; Goulielmakis, E. Synthesized Light Transients. *Science* **2011**, *334*, 195–200.

(96) Rohringer, N.; Santra, R. Multichannel Coherence in Strong-Field Ionization. *Phys. Rev. A* **2009**, *79*, 053402-1–053402-10

(97) Wang, H.; Chini, M.; Chen, S.; Zhang, C.-H.; He, F.; Cheng, Y.; Wu, Y.; Thumm, U.; Chang, Z. Attosecond Time-Resolved Autoionization of Argon. *Phys. Rev. Lett*. **2010**, 105, 143002-1–143002-4.

(98) Remetter, T.; Johnsson, P.; Mauritsson, J.; Varjú, K.; Ni, Y.; Lépine, F.; Gustafsson, E.; Kling, M.; Khan, J.; López-Martens, R.; Schafer, K. J.; Vrakking, M. J. J.; L'Huillier, A. Attosecond Electron Wave Packet Interferometry. *Nature Phys*. **2006**, *2*, 323–326.

(99) Johnsson, P.; Mauritsson, J.; Remetter, T.; L'Huillier, A.; Schafer, K. J. Attosecond Control of Ionization by Wave-Packet Interference. *Phys. Rev. Lett*. **2007**, *99*, 233001-1–233001-4.

(100) Holler, M.; Schapper, F.; Gallmann, L.; Keller, U. Attosecond Electron Wave-Packet Interference Observed by Transient Absorption. *Phys. Rev. Lett*. **2011**, *106*, 123601-1–123601-4.

(101) Reiter, F.; Graf, U.; Serebryannikov, E. E.; Schweinberger, W.; Fiess, M.; Schultze, M.; Azzeer, A. M.; Kienberger, R.; Krausz, F.; Zheltikov, A. M.; Goulielmakis, E. Route to Attosecond Nonlinear Spectroscopy. *Phys. Rev. Lett.* **2010**, *105*, 243902-1–243902-4.

(102) Mignolet, B.; Gijsbertsen, A.; Vrakking, M. J. J.; Levine, R. D.; Remacle, F. Stereocontrol of Attosecond Time-Scale Electron Dynamics in ABCU using Ultrafast Laser Pulses: A Computational Study. *Phys. Chem. Chem. Phys*. **2011**, *13*, 8331–8344.

(103) Barth, I.; Manz, J.; Shigeta, Y.; Yagi, K. Unidirectional Electronic Ring Current Driven by a Few Cycle Circularly Polarized Laser Pulse: Quantum Model Simulations for Mg-Porphyrin. *J. Am. Chem. Soc.* **2006**, *128*, 7043–7049.

(104) Remacle, F.; Nest, M.; Levine, R. D. Laser Steered Ultrafast Quantum Dynamics of Electrons in LiH. *Phys. Rev. Lett.* **2007**, *99*, 183902-1–183902-4.

(105) Seres, E.; Seres, J.; Spielmann, C. X-Ray Absorption Spectroscopy in the keV Range with Laser Generated High Harmonic Radiation. *Appl. Phys. Lett.* **2006**, *89*, 181919-1–181919-3.

(106) Mashiko, H.; Gilbertson, S.; Chini, M.; Feng, X.; Yun, C.; Wang, H.; Khan, S. D.; Chen, S.; Chang, Z. Extreme Ultraviolet Supercontinua Supporting Pulse Durations of Less Than One Atomic Unit of Time. *Opt. Lett.* **2009**, *34*, 3337–3339.

(107) Baker, S.; Robinson, J. S.; Haworth, C. A.; Teng, H.; Smith, R. A.; Chirala, C. C.; Lein, M.; Tisch, J. W. G.; Marangos, J. P. Probing Proton Dynamics in Molecules on an Attosecond Time Scale. *Science* **2006**, *312*, 424–427.

(108) Seres, J.; Seres, E.; Hochhaus, D.; Ecker, B.; Zimmer, D.; Bagnoud, V.; Kuehl, T.; Spielmann, C. Laser-Driven Amplification of Soft X-Rays by Parametric Stimulated Emission in Neutral Gases. *Nature Phys.* **2010**, *6*, 455–461.

(109) Popmintchev, T.; Chen, M.-C., Popmintchev, D.; Arpin, P.; Brown, S.; Ališauskas, S.; Andriukaitis, G.; Balčiunas, T.; Mücke, O. D.; Pugzyls, A.; Baltuška, A.; Shim, B.; Schrauth, S. E.; Gaeta, A.; Hernández-García, C.; Plaja, L.; Becker, A.; Jaron-Becker, A.; Murnane, M. M.; Kapteyn, H. C. Bright Coherent Ultrahigh Harmonics in the keV X-Ray Regime from Mid-Infrared Femtosecond Lasers. *Science* **2012**, *336*, 1287–1291.

(110) Zholents, A. A.; Fawley, W. M. Proposal for Intense Attosecond Radiation from an X-Ray Free-Electron Laser. *Phys. Rev. Lett.* **2004**, *92*, 224801-1–224801-4.

(111) Breidbach, J.; Cederbaum, L. S. Universal Attosecond Response to the Removal of an Electron. *Phys. Rev. Lett.* **2005**, *94*, 033901-1–033901-4.

(112) Remacle, F.; Levine, R. D. An Electronic Time Scale in Chemistry. *Proc. Natl. Acad. Sci. USA* **2006**, *103*, 6793–6798.

Quotes to highlight

p. 5: The recent advent of femtosecond and attosecond x-ray pulses now allows time-resolved x-ray absorption to approach time scales that are commensurate with nuclear and even electronic motion.

p. 7: These experiments yield some of the earliest information on state-resolved populations and dynamics in strong-field phenomena.

p. 20: This result not only demonstrates the feasibility of performing transient absorption spectroscopy with attosecond time resolution, it also points to the possibility of employing strong-field ionization as a general strategy for initiating nonstationary electron dynamics.

p. 23: Such experiments promise access to the holy grail of attosecond science – the ability to observe correlated electron dynamics in real time.